Synchronization of unidirectionally coupled Mackey-Glass analog circuits with frequency bandwidth limitations

Min-Young Kim,[1,2,*] Christopher Sramek,[1] Atsushi Uchida,[1] and Rajarshi Roy[1,2,3]
[1]*Institute for Research in Electronics and Applied Physics, University of Maryland, College Park, Maryland 20742, USA*
[2]*Department of Physics, University of Maryland, College Park, Maryland 20742, USA*
[3]*Institute for Physical Science and Technology, University of Maryland, College Park, Maryland 20742, USA*
(Received 13 February 2006; revised manuscript received 13 June 2006; published 27 July 2006)

Synchronization of chaotic systems has been studied extensively, and especially, the possible applications to the communication systems motivated many research areas. We demonstrate the effect of the frequency bandwidth limitations in the communication channel on the synchronization of two unidirectionally coupled Mackey-Glass (MG) analog circuits, both numerically and experimentally. MG system is known to generate high dimensional chaotic signals. The chaotic signal generated from the drive MG system is modified by a low pass filter and is then transmitted to the response MG system. Our results show that the inclusion of the dominant frequency component of the original drive signals is crucial to achieve synchronization between the drive and response circuits. The maximum cross correlation and the corresponding time shift reveal that the frequency-dependent coupling introduced by the low pass filtering effect in the communication channel change the quality of synchronization.

DOI: 10.1103/PhysRevE.74.016211 PACS number(s): 05.45.−a

Since Mackey and Glass suggested a mathematical model to describe the dynamics of a physiological control system [1], there have been numerous studies on the Mackey-Glass model [2–10]. The Mackey-Glass model is described by a first-order delay differential equation

$$\frac{dx}{dt} = \frac{ax_\tau}{1 + x_\tau^n} - bx, \tag{1}$$

where x is the variable of interest at time t, $x_\tau = x(t-\tau)$ is the time-delayed variable with a fixed delay time τ, and a, b, and n are constant parameters. For most of the numerical studies, the delay time is used as a control parameter with the parameter values of $a=0.2$, $b=0.1$, and $n=10$. It is known that the system shows steady, periodic, and chaotic dynamics as the delay time is varied [2]. It is also known that the dimension of chaotic dynamics increases linearly proportional to the delay time [2].

The synchronization of chaotic systems has been investigated extensively because of its potential applications in communication [11–15]. Practically, however, there exist transmission channel effects, such as bandwidth limitation, phase distortion, amplitude attenuation, and channel noise, and there have been few studies on the synchronization of chaotic systems with transformation due to the channel [16,17]. In this paper, we investigate the properties of synchronization when the signal from the drive system is altered by the frequency bandwidth limitations in the communication channel. Two unidirectionally coupled Mackey-Glass analog circuits are used as a drive and a response circuit, as shown in Fig. 1(a). A chaotic signal generated from the drive circuit passes through a low pass filter (LPF) in the channel and becomes an input to the response circuit. An open-loop configuration is used for the response circuit in order to achieve a better quality of synchronization of chaos.

An electronic circuit imitating the behavior of the MG system is constructed based on Ref. [7] with slight modifications. As shown in Fig. 1(a), each circuit contains a delay unit, a nonlinear device (ND), and a fixed RC filter, as demonstrated by Namajunas *et al.* [7]. The nonlinear device consists of coupled junction field effect transistors (JFETs, 2N5461 and 2N5458), and Fig. 1(b) plots the output vs input voltage transfer curve from experimentally obtained data [18]. The delay unit is an LC network with the cutoff frequency of around 40 kHz. The delay resolution is 6.86 μs,

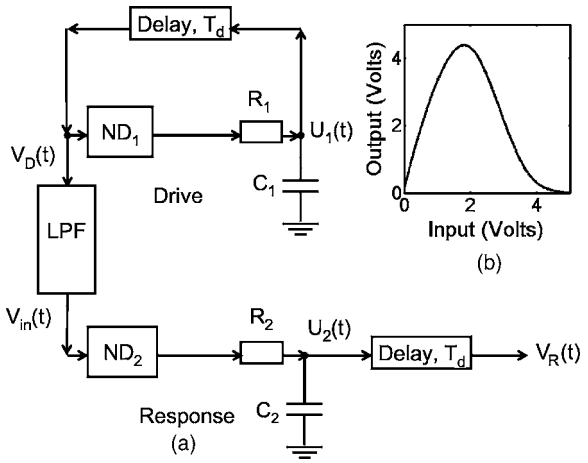

FIG. 1. (a) Schematic diagram of two unidirectionally coupled Mackey-Glass analog circuits with an open-loop configuration for the response circuit. ND_1 and ND_2 are nonlinear devices; T_d is delay time in seconds; R_1 and R_2 are resistors; C_1 and C_2 are capacitors; LPF is a low pass filter in the communication channel; U_1 and U_2 are the voltage across the capacitor C_1 and the voltage across the capacitor C_2, respectively. $V_D(t)$ is the output from the drive circuit, and $V_R(t)$ is the output from the response circuit. $V_{in}(t)$ is the input to the response circuit. (b) The nonlinear device characteristic curve.

*Electronic address: mmyykim@glue.umd.edu

and the fixed delay of ~180 μs is used for our experiments. The parameters of each fixed RC filter in Fig. 1(a) are matched closely with $R_1=R_2=2.35$ kΩ, $C_1=C_2=11$ nF; thus, the time constant is $R_1C_1=R_2C_2 \sim 26$ μs and the corresponding cutoff frequency is 6.1 kHz.

From the circuit model, the voltages $U_1(t)$ and $U_2(t)$ can be described by

$$R_1C_1\frac{dU_1(t)}{dt} = \mathrm{ND}_1[cU_1(t-T_d)] - U_1(t), \tag{2}$$

$$R_2C_2\frac{dU_2(t)}{dt} = \mathrm{ND}_2[V_{\mathrm{in}}(t)] - U_2(t), \tag{3}$$

where R_1 and R_2 are resistances, C_1 and C_2 are capacitances, T_d is the delay time, and c is the feedback gain on the delay loop. ND_1 and ND_2 are the transfer functions of each nonlinear device. $V_{\mathrm{in}}(t)$ is the input to the response circuit. Without LPF in the channel, $V_{\mathrm{in}}(t)=AcU_1(t-T_d)$, where A denotes the dc attenuation. An LPF in the channel, on the other hand, creates a frequency-dependent attenuation.

We introduce dimensionless variables and dimensionless parameters

$$\frac{cU_1(t)}{U_{1s}} = x(t), \quad \frac{cU_2(t)}{U_{1s}} = y(t), \quad \frac{V_{\mathrm{in}}(t)}{U_{1s}} = y_{\mathrm{in}}(t), \tag{4}$$

$$\frac{t}{R_1C_1} = t', \quad \frac{T_d}{R_1C_1} = \tau, \quad \frac{R_2C_2}{R_1C_1} = \frac{1}{b}, \tag{5}$$

where $x(t)$ is the drive signal, $y(t)$ is the response signal, $y_{\mathrm{in}}(t)$ is the input to the response system, and b corresponds to the mismatch in RC constants. Nonzero U_{1s} is chosen such that $\mathrm{ND}_1\ (U_{1s})=U_{1s}$. The coupled equations become

$$\frac{dx}{dt'} = c\lambda_1(x_\tau) - x, \tag{6}$$

$$\frac{dy}{dt'} = b[c\lambda_2(y_{\mathrm{in}}) - y], \tag{7}$$

with $\lambda_1(x)=\mathrm{ND}_1/U_{1s}$, $\lambda_2(x)=\mathrm{ND}_2/U_{1s}$. Since each equation is isomorphic to Eq. (1), we approximate $\lambda_1(x)=\lambda_2(x)=2x/(1+x^{10})$ for the numerical simulations, assuming identical transfer characteristics for both circuits.

In our experiment, the delay T_d is fixed at ~180 μs and the feedback gain c is used as a control parameter [19]. By increasing the feedback gain experimentally, we can observe that the dynamics of system change from steady through periodic to chaotic state. Figure 2(a) shows the chaotic time series taken from the drive circuit. The corresponding power spectrum in Fig. 2(b) shows periodic peaks in addition to the broadband spectrum. The dominant peak is located at the fundamental frequency of the delayed feedback loop, $f_1=2.7$ kHz$\sim 1/(2T_d)$. Figure 2(c) is the phase portrait of the signal $V_D(t)$ vs the delayed signal $V_D(t-T_d)$. All subsequent experimental results presented in this paper are obtained using the same feedback gain as in Fig. 2.

To investigate the properties of synchronization with the

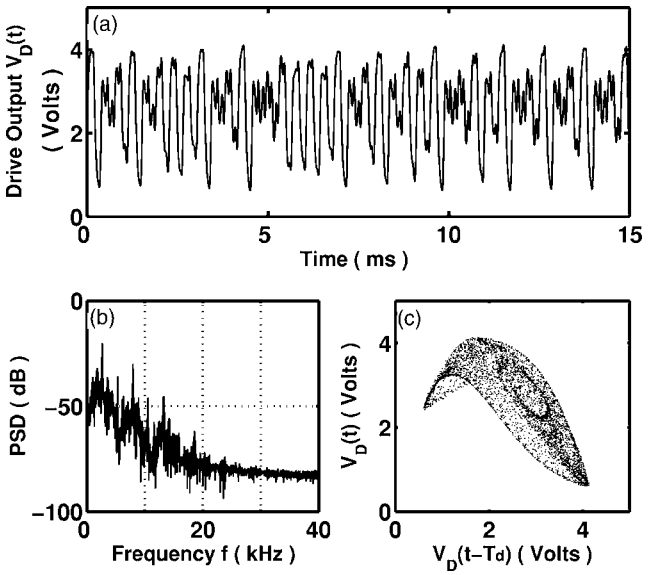

FIG. 2. Experimental chaos. (a) The time series, (b) power spectral density (PSD) in decibels, and (c) phase portrait generated by a Mackey-Glass analog circuit. The sampling time is 10 μs. The PSD is obtained using the FFT algorithm and is an average of PSDs from five consecutive 4096-point time series.

frequency bandwidth limitations in the communication channel, we used two types of low pass filter, a passive RC filter and an active two-pole Chebyshev filter [20], and varied the cutoff frequency by replacing resistor and capacitor components. The 3 dB cutoff frequency, f_c, was approximated in each case. There was no dc gain adjustment made for an RC filter, whereas for an Chebyshev filter, the dc gain was adjusted every time f_c was changed.

Figure 3 shows the time series from the drive and response circuits (left column), and the phase portraits from the response circuit (right column) at different conditions of LPF in the communication channel. Without any filter (top), the response system exactly follows the drive system and reconstructs the same phase portrait as shown in Fig. 2(c). With a passive RC filter at a cutoff frequency of $f_c=12.1$ kHz ($f_c>f_1$) in Figs. 3(c) and 3(d), the fast oscillations are removed in the response system, but the phase portrait is still similar to that of the drive system. With an RC filter at a cutoff frequency of $f_c=125$ Hz ($f_c<f_1$) in Figs. 3(e) and 3(f), the distortion in the phase portrait is clearly observed. In both cases with an RC filter, the response system follows the drive system with a constant time lag at reduced amplitude.

For the comparison of two time series, we calculated the time-shifted cross-correlation coefficient between the drive output and the response output

$$C(\Delta t) = \frac{\langle [V_{\mathrm{D}}(t) - \langle V_{\mathrm{D}}(t)\rangle][V_{\mathrm{R}}(t+\Delta t) - \langle V_{\mathrm{R}}(t)\rangle]\rangle}{\sqrt{\langle |V_{\mathrm{D}}(t) - \langle V_{\mathrm{D}}(t)\rangle|^2\rangle\langle |V_{\mathrm{R}}(t) - \langle V_{\mathrm{R}}(t)\rangle|^2\rangle}}, \tag{8}$$

where angular brackets denotes a time average. Figures 4(a) and 4(b) show the color map of the cross-correlation coefficient calculated at different values of a cutoff frequency, with an RC filter in Fig. 4(a) and with a Chebyshev filter in Fig.

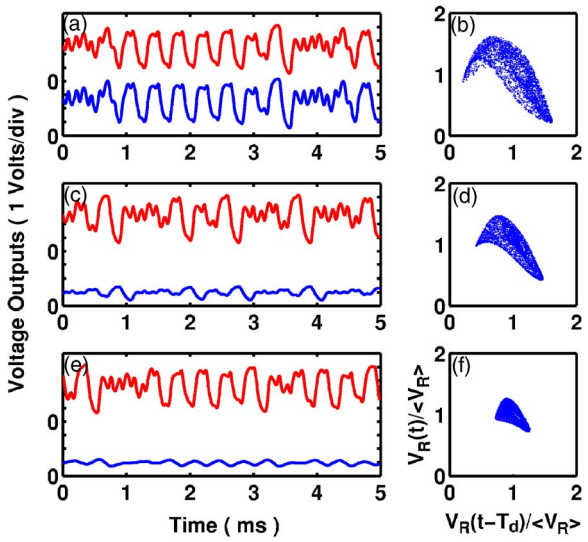

FIG. 3. (Color online) Experimental time series and phase portraits. Left column, time series from the drive circuit (upper traces) and from the response circuit (lower traces); right column, phase portraits reconstructed from the response output normalized to its mean value. From top to bottom, no filter, an RC filter with a cutoff frequency of 12.1 kHz, an RC filter with a cutoff frequency of 125 Hz, respectively, is used in the communication channel.

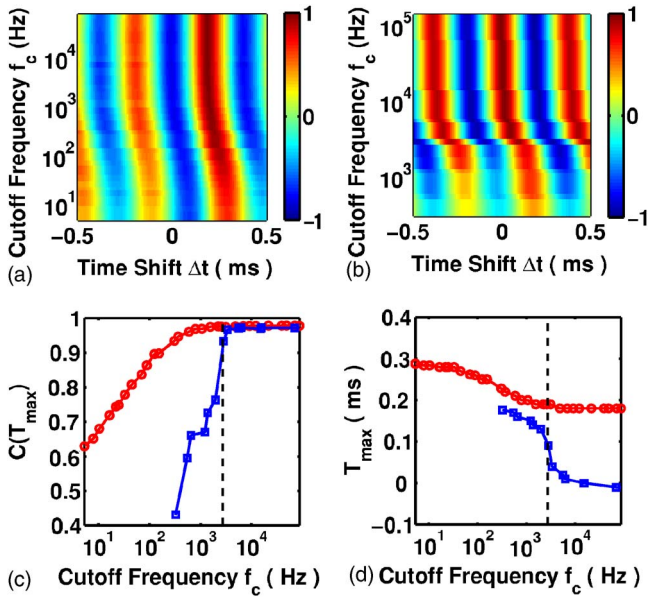

FIG. 4. (Color online) Experimental observations. (a) The color map of the shifted cross-correlation coefficient $C(\Delta t)$ [Eq. (8)] with an RC filter in the channel, at different values of the cutoff frequency f_c. (b) Same plot as (a) but with a two-pole Chebyshev filter in the channel. (c) The maximum cross-correlation coefficient vs f_c and (d) the corresponding time shift at maximum correlation, $T_{\max}$, measured in milliseconds (circles for RC filters and squares for two-pole Chebyshev filters). The vertical lines are located at the fundamental frequency $f_1=2.7$ kHz.

4(b). For $f_c \gg f_1$, the local extrema of $C(\Delta t)$ occur at the multiples of T_d with an alternating maximum and minimum for both types of filter. For $f_c \ll f_1$, this alternating band structure is shifted by $T_d/2$ with an RC filter, and by T_d with a Chebyshev filter.

The dependence of the maximum cross-correlation $C(T_{\max})$ and the corresponding time shift $T_{\max}$ on the cutoff frequency is plotted in Figs. 4(c) and 4(d) [21]. The vertical lines are located at the dominant peak of the power spectrum of the chaotic drive signal, i.e., $f_1=2.7$ kHz for our experimental setup. The maximum correlation is reduced dramatically for $f_c<f_1$ and is saturated for $f_c>f_1$. In other words, the inclusion of the frequency components up to the dominant frequency is very important to achieve synchronization of the response output with the drive output. Once this condition is satisfied, i.e., if $f_c>f_1$, the higher frequency components with $f>f_1$ do not significantly affect the quality of synchronization in our system. In addition, $T_{\max}$ also shows transition at around the fundamental frequency. As the cutoff frequency f_c decreases below f_1, $T_{\max}$ increases from 180 to 290 μs with an RC filter, and from 0 to 180 μs with a Chebyshev filter.

To better understand the experimental observations, we explore the numerical simulations by integrating Eqs. (6) and (7) with $y_{\text{in}}(t')=A\times\text{IFFT}\{H(f)\times\text{FFT}[x(t'-\tau)]\}$. A fixed-step fourth-order Runge-Kutta method is used with an integration time step $\Delta t'=0.005$, and the linear interpolation is used for the required two midpoint evaluations of the delayed variables. First, we generate the drive signal $x(t')$ starting with a constant initial condition ($x_0=0.9$) on $(-\tau,0)$. After a transient period ($t'>200\tau$), the delayed drive signal $x(t'-\tau)$ in a time window of 750τ is fast Fourier transformed (FFT), multiplied by the transfer function of a low pass filter in the channel $H(f)$, and inverse fast Fourier transformed (IFFT) to obtain the input signal $y_{\text{in}}(t')$ at time t'. The transfer function of an RC filter is $H_{\text{RC}}(f)=1/(jf/f_c+1)$ and that of an active two-pole Chebyshev filter is $H_{\text{CB}}(f)=1/[-c_1(f/f_c)^2+jc_2(f/f_c)+1]$ where $c_1=1.4018$ and $c_2=1.0490$. The response signal $y(t')$ is then integrated from Eq. (7) using $y_{\text{in}}(t')$ as an input signal with a zero initial condition. The value of the feedback gain parameter c is chosen such that the power spectrum of numerical time series matches that of experimental time series.

In Fig. 5, we calculate the maximum values of the cross-correlation coefficient $C(T_{\max})$ and the corresponding time shift $T_{\max}$, between numerically obtained drive and response signals, $x(t')$ and $y(t')$, at different values of the cutoff frequency. Without dc attenuation ($A=1$), for the cutoff frequency much higher than the fundamental frequency ($f_c \gg f_1$), the maximum coefficient $C(T_{\max})$ is equal to 1 and $T_{\max}=0$, i.e., the response system is synchronized to the drive system. $T_{\max}$ increases as f_c decreases below f_1, approaching $T_{\max}=T_d$ with the Chebyshev filter (stars) and $T_{\max}=T_d/2$ with an RC filter (triangles). The corresponding maximum correlation coefficient reduces as f_c decreases below f_1, which is more dramatic with a Chebyshev filter. On the other hand, with dc attenuation ($A=0.5$), $T_{\max}$ is shifted upward by an amount of T_d for both filters, whereas $C(T_{\max})$ still looks similar to the case of $A=1$. For $f_c \gg f_1$, $C(T_{\max})=1$ with $T_{\max}=T_d$, where the response system is linearly modulated by the input signal, which is the low pass filtered, delayed drive signal.

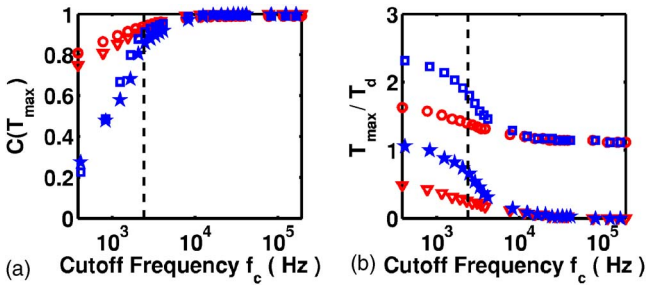

FIG. 5. (Color online) Numerical results. (a) The maximum cross-correlation coefficient $C(T_{\max})$ vs the cutoff frequency f_c and (b) the corresponding time shift at maximum correlation normalized to the delay time. The circles are obtained with an RC filter at $A=0.5$, the triangles with an RC filter at $A=1.0$, the squares with an Chebyshev filter at $A=0.5$, and the stars with an Chebyshev filter at $A=1.0$. The vertical lines are located at the fundamental frequency f_1 ($b=1$, $c=0.72$, $\tau=7$).

As mentioned earlier, the dc attenuation in the communication channel was compensated for a Chebyshev filter, whereas the dc attenuation with an RC filter was not compensated in our experiments. Therefore, the numerical simulations of the Chebyshev filter without dc attenuation and the RC filter with dc attenuation, closely approximate the experimental observations. The transition in $C(T_{\max})$ and $T_{\max}$ from Fig. 5 occurs at a frequency higher than f_1 for both filters, which shows discrepancy from the experimental transition points. A more precise determination of the cutoff frequency and a more accurate compensation of the dc attenuation in the experiments, as well as an improvement of the filtering in the numerical simulations, will be necessary to solve the discrepancy.

The dependence of $T_{\max}$ on the cutoff frequency turns out to be induced by the phase distortion due to a low pass filter in the communication channel [22]. Intuitively, since most of the power in the original drive signal is carried by the dominant frequency component, the filtered signal is shifted in time from the original signal, by the amount of the phase distortion occurring at the dominant frequency.

In summary, using a low pass filter in the communication channel, we studied the effect of a frequency-dependent coupling on the synchronization of two unidirectionally coupled Mackey-Glass analog circuits. The inclusion of the frequency components up to the fundamental frequency of the drive signal is crucial to achieve synchronization. In addition, both the dc attenuation and the phase distortion due to the low pass filtering effect in the channel play important roles to determine the quality of synchronization in the response system.

The authors acknowledge Vasily Dronov for building the Mackey-Glass analog circuits. We also acknowledge the TRENDS National Science Foundation REU Program at the University of Maryland.

[1] M. C. Mackey and L. Glass, Science **197**, 287 (1977).
[2] J. D. Farmer, Physica D **4**, 366 (1982).
[3] P. Grassberger and I. Procaccia, Physica D **9**, 189 (1983).
[4] J. Losson, M. C. Mackey, and A. Longtin, Chaos **3**, 167 (1993).
[5] B. Mensour and A. Longtin, Physica D **113**, 1 (1998).
[6] B. Mensour and A. Longtin, Phys. Rev. E **58**, 410 (1998).
[7] A. Namajunas, K. Pyragas, and A. Tamasevicius, Phys. Lett. A **201**, 42 (1995).
[8] A. Namajunas, K. Pyragas, and A. Tamasevicius, Phys. Lett. A **204**, 255 (1995).
[9] S. Boccaletti, D. L. Valladares, J. Kurths, D. Maza, and H. Mancini, Phys. Rev. E **61**, 3712 (2000).
[10] H. U. Voss, Int. J. Bifurcation Chaos Appl. Sci. Eng. **12**, 1619 (2002).
[11] L. M. Pecora and T. L. Carroll, Phys. Rev. Lett. **64**, 821 (1990).
[12] L. Kocarev, K. S. Halle, K. Eckert, L. O. Chua, and U. Parlitz, Int. J. Bifurcation Chaos Appl. Sci. Eng. **2**, 709 (1992).
[13] K. M. Cuomo and A. V. Oppenheim, Phys. Rev. Lett. **71**, 65 (1993).
[14] G. D. VanWiggeren and R. Roy, Science **279**, 1198 (1998).
[15] S. Tang and J. M. Liu, IEEE J. Quantum Electron. **39**, 708 (2003).
[16] T. L. Carroll, Phys. Rev. E **50**, 2580 (1994); IEEE Trans. Circuits Syst., I: Fundam. Theory Appl. **42**, 105 (1995); Phys. Rev. E **53**, 3117 (1996).
[17] N. J. Corron and D. W. Hahs, IEEE Trans. Circuits Syst., I: Fundam. Theory Appl. **44**, 373 (1997).
[18] Because of the polarity of the coupled JFETs and inverted OP amps used in the circuits (not shown), V_D, V_{in}, and V_R were negative all the times, and we simply used absolute values of data to plot Figs. 1(b), 2, and 3.
[19] The gain of an inverted OP amp in the circuits not shown is controlled by a potentiometer, resulting in a change in the net feedback gain of each citcuit.
[20] J. Millman and A. Grabel, *Microelectronics*, 2nd ed. (McGraw-Hill, Singapore, 1987), Chap. 16.
[21] A two-channel oscilloscope (GageScope CS1450) recorded 4096 data points from both circuits simultaneously, at 10^5 samples per second for a single time window. The average values of C ($T_{\max}$) and $T_{\max}$ were calculated from five time windows at a given cutoff frequency, f_c. Error bars are not shown since the size was comparable to the marker size of each data point.
[22] M.-Y. Kim, Ph. D. thesis, University of Maryland, College Park, 2005 (unpublished).